Study of Glycerol as an Additive in Ni-Mo Electrodeposition

Javan Grisente dos Reis da Costa[a]* [ID], **Cláudia Lisiane Fanezi da Rocha[b]** [ID],

Luiz Rogério Pinho de Andrade Lima[b] [ID], **Daniel Veras Ribeiro[b]** [ID], **Carlos Alberto Caldas de Souza[a]** [ID]

[a]*Universidade Federal da Bahia, Programa de Pós-Graduação em Engenharia Química - PPEQ, Salvador, BA, Brasil.*
[b]*Universidade Federal da Bahia, Departamento de Ciência e Tecnologia dos Materiais - DCTM, Salvador, BA, Brasil.*

This paper evaluates the effect of adding glycerol to the electrodeposition bath on the deposition efficiency and characteristics of Ni-Mo coating in concentrations ranging from 0.07 to 0.82 mol.L^{-1}. Evaluation of the corrosion resistance was performed by means of weight loss tests in four different periods of immersion. Electrochemical techniques, such as obtaining polarization curves, linear polarization resistance, corrosion current density, corrosion potential, and electrochemical impedance spectroscopy were applied. Corrosion measurements were obtained in 0.5 mol.L^{-1} NaCl acid solution and 0.5 mol.L^{-1} NaOH alkaline solution. The morphology and microstructures of electrodeposited were analyzed using Scanning Electron Microscopy and Spectrometry X-Ray Diffraction. The effect of glycerol on Ni-Mo hardness was evaluated by Vickers microhardness measurements. The presence of glycerol in the electrodeposition bath increased the grain size and decreased the hardness of the coating. However, it promoted the formation of a more compact and less porous coating, increasing the corrosion resistance of the coating. Moreover, the addition of 0.82 mol.L^{-1} glycerol increases current ef0ficiency, thereby reducing the amount of energy consumed during electroplating.

Keywords: *Corrosion, glycerol, electroplating, Nickel, Molybdenum.*

1. Introduction

Nickel coatings obtained by electroplating are mainly used in decorative applications. However, they are also used in applications where corrosion resistance and / or abrasion wear is important, such as in coating bolts and brake components. The addition of Mo to Ni significantly increases corrosion resistance, hardness and wear resistance making it promising to use Ni-Mo coating in place of hard chrome coating[1-3]. In addition to high thermal stability, high hardness, wear resistance and corrosion resistance, Ni-Mo coating is an environmentally friendly alternative to hard chrome[4]. The use of hard chrome coatings is now restricted due to the presence of hexavalent chromium ions in the bath deposition which are toxic and carcinogenic. Ni-Mo coating also has low overpotential for the hydrogen evolution reaction which makes it possible to use this coating as a cathode for hydrogen production reaction[5-8].

It has been found[9] that it is not possible to deposit Ni-Mo alloys from aqueous solutions containing only Ni^{2+} and MoO$_4^{2-}$ without the use of a complexing agent, which is a chemical agent that aids in the dissolution of metal ions. Ni-Mo electroplating has been tested with different complexing agents such as acetate, tartrate, pyrophosphate, citrate and ammonia, but only citrate and pyrophosphate appear to be the most promising in terms of quality, adhesion and mechanical properties[9].

Ni–Mo coatings with 6.3–22 at.% Mo consist of face-centered cubic solid solution with Mo atoms dissolved in the lattice of Ni[10]. However, with the addition of Mo, the degree of crystallinity decreases and the coating exhibits a quasi-amorphous structure for a higher amount of Mo. The Ni-Mo coating grains have a nanocrystalline dimension, which decreases with the increase in Mo content[10]. The effect of Mo on the refining of Ni-Mo alloy grains is attributed to the segregation of this solute in grain boundaries, an effect similar to that of W in Ni-W coating. This achievement is related to the reduction of the energy of the grain boundary, resulting in the decrease of the driving force for grain growth[11]. Yet for a Mo content of 25 at.%, the coating exhibits the presence of cracks which become more predominant with increasing Mo content[12,13]. The presence of these cracks is caused by the tension resulting from the addition of Mo, and their propagation occurs in order to release the internal stress[14]. In addition to increasing internal stresses and promoting grain refining, the presence of Mo also reduces the roughness of the coating surface, making it smoother[10].

The addition of Mo to an Ni coating increases the corrosion resistance in sulfuric acids and in neutral chloride solutions, particularly in seawater. However, from a certain

Mo content any further increase in Mo content will promote the occurrence of pitting resulting in a decrease in corrosion resistance, which is attributed to the decrease in grain size and the presence of an internal stress[4,10,15].

The effect of the addition of Mo on improving corrosion resistance is attributed[4,10,15] to the formation of a protective oxide film and a higher Mo content makes this film more stable thereby increasing the corrosion resistance of the coating. Oxidation products such as NiO, MoO_2 and MoO_3 can form a thin passive film to protect the coating from corrosion[10].

It has been proposed[16-18] that increasing the Mo content causes a decrease in grain size and from a certain concentration of this element the grain refining effect predominates which decreases the corrosion resistance of the coating. This grain refining effect is related to the increased grain boundary area per coating volume, and as the grain boundary acts as the preferred corrosion site, corrosion resistance decreases with grain refining. However, if the factor that causes grain refining results in a smoother surface, the corrosion resistance of the coating may increase even as the grain size decreases[18]. It has also been proposed[4] that the higher Mo content causes internal stresses in the coating, and from a given content of this element these tensions cause the presence of cracks, which cause the passive film to break, thus decreasing the corrosion resistance.

The works published in the literature have demonstrated that the optimal Mo content in the corrosion resistance of Ni-Mo coating depends on the composition of the aggressive medium. In a study[10] on the corrosion resistance of Ni-Mo coating with different Mo content (6.3, 12.6, 16.7, 19.1, and 22 at.%) It was found that the 16.7 at.% Mo coating exhibits greater corrosion resistance in 0.5 mol. L^{-1} H_2SO_4. After 24 hours of immersion in the solutions 3.5 wt.% NaCl and 3 v / v% HCl, in which Ni-Mo coating with 7, 15, 20, 23, 25, 27, 30, 35, and 42 wt.% Mo was analyzed, an optimum content of 15 wt% Mo was found[12]. According to the results obtained by Halim et al.[15], in a 0.5 mol.L^{-1} NaOH solution Ni-Mo coating containing 15% wt. Mo has a higher corrosion resistance than Mo-containing coating between 11% wt. and 32% wt. However, the effect of Mo content on the corrosion resistance of Ni-Mo coating depends on the contact time of the coating with the corrosive medium. Laszczyńska et al.[4] found that after 24 hours of immersion in 0.5 mol.L^{-1} NaCl solution the Ni-Mo coating containing 26% wt. Mo has a higher corrosion resistance than Mo containing coatings by 11% wt. and 32% wt. According to these authors, after a long period of exposure in 0.5 mol.L^{-1} NaCl solution, the formation of a passive film has a crucial influence on the corrosion velocity of a high Mo content Ni-Mo coating. However, for higher Mo contents such as 32% wt. the high internal tension causes cracks to be present.

The increased corrosion resistance of an Ni-Mo coating has a significant economic impact on its application. The amount of molybdate in the deposition bath required for the corrosion resistance of the coating to be adequate is lower.

One of the procedures that can increase the corrosion resistance of this coating is the addition of additives such as polythiophene (PTh) polymer and ceramic nanoparticles. Among the ceramic nanoparticles are montmorillonite (MMT), Al_2O_3, SiC and TiN, as well as graphene oxide (GO) nanosheets. The increased corrosion resistance of Ni-Mo with the addition of PTh is attributed to the presence of PTh on the coating surface which results in decreased active surface area of the corrosion susceptible electrode[19]. However, it is not clear how the presence of organic additives affects Ni-Mo coating characteristics especially when they are incorporated into the coating.

The improvement of the corrosion resistance of Ni-Mo due to the addition of ceramic nanoparticles is attributed to the following factors: performance of nanoparticles as a physical barrier with the consequent decrease in the active surface area[19-21]; filling of cracks and holes by nanoparticles[20]; and prevention of localized corrosion with the formation of microcell corrosion[21]. Regarding the addition of GO nanosheets, it has been proposed[22] that the presence of these nanosheets constitutes a barrier with low permeability that covers the deposit surface inhibiting the penetration of corrosive substances such as Cl^- and oxygen.

As with corrosion resistance, there is an optimum Mo content in the Ni-Mo coating in which the coating hardness is maximum. It has been found[10] that in as – deposited Ni – Mo coatings with 6.3–22 at.% Mo the hardness is maximum at 16.7 at.% Mo, and decreases with increasing Mo content. The increase in hardness with the increase in the Mo content in the Ni-Mo coating is attributed to the grain refining caused by the addition of Mo (Hall – Petch effect). The decrease in the size of the grains results in a larger volumetric fraction of the grain contour, which acts as an obstacle to the movement of discrepancies. However, below a certain critical grain size with nanocrystalline dimension, 7.9 nm to 16.7 at.% Mo, the reverse Hall – Petch effect occurs, that is, the hardness decreases with the grain refining[10].

Due to the high cost of ceramic nanoparticles and insufficient knowledge of the effect of organic additives on the characteristics of Ni-Mo coating, it is interesting to investigate the effect of organic additives on the characteristics of Ni-Mo coating obtained by electroplating. The addition of glycerol in electrodeposited coating has attracted attention because it is a product obtained from the transformation of vegetable oil into biodiesel, thus is an abundant and low-cost product[22]. The addition of glycerol has been found to increase the corrosion resistance of Zn[23] and Zn-Ni[24] coatings. It has also been found[25] that the addition of glycerol in Ni coating inhibits crack formation. However, there is no information on the effect of the addition of glycerol on Ni-Mo coating.

The present work aims to analyze the effect of the addition of glycerol in the deposition bath on Ni-Mo coating characteristics, including corrosion resistance, microhardness, surface roughness and microstructure. Corrosion resistance is evaluated in both acid and alkaline environments by mass loss tests and electrochemical techniques, such as obtaining polarization curves, linear polarization resistance (Rp) and electrochemical impedance spectroscopy (EIS). The structural evaluation of the deposit is made using XRD and SEM techniques.

The coating electrodeposition current is an important factor in the cost of the electroplating process as it is related to the amount of electricity consumed during the process. However, studies on the effect of additives on corrosion resistance of Ni-Mo coating generally do not analyze the

effect of these additives on current efficiency. Therefore, the effect of the addition of glycerol on the deposition efficiency of Ni-Mo coating is also evaluated in the present work.

2. Experimental Procedure

The composition of the deposition bath is listed in Table 1. Three concentrations of glycerol were added to the electrodeposition bath (0.07, 0.27 and 0.82 mol.L^{-1}). With the presence of glycerol, the deposition bath at pH 10 was maintained at this pH with the addition of ammonium hydroxide (NH$_4$OH). The addition of amounts of glycerol greater than 0.82 mol.L^{-1} was found to result in a non-adherent coating to the substrate.

Ni-Mo coatings were electrodeposited onto a carbon steel AISI 1020 substrate embedded in polymeric resin. The parameters used in the galvanostatic deposition were: room temperature (25ºC); without agitation; current density 35 mA.cm^{-2}; graphite bar used as anode; electrodeposition time 9,8 min; 5 µm thick coating.

To compare the hardness results, a Ni coating was also obtained under the following conditions: room temperature (25ºC); without agitation; current density 10 mA.cm^{-2}; graphite bar used as anode; pH 5; electrodeposition time 17,4 min; 5 µm thick coating. A deposition bath containing 120 g.L^{-1} NiSO$_4$, 30g.L^{-1} NiCl$_2$, and 45g.L^{-1} H$_3$BO$_3$[26]

Corrosion resistance was evaluated in 0.5 mol.L^{-1} NaCl and 0.5 mol.L^{-1} NaOH solutions, through measurements of mass loss and electrochemical techniques. In the measurements of mass loss, the deposits obtained in the absence and in the presence of different concentrations of glycerol were immersed for several periods of time in the corrosive solution (24, 48, and 72 hours). All values were obtained in triplicate. The cleaning of the surface of the Ni-Mo coating after immersion in a corrosive solution was done with a solution of glycine (aminoacetic acid - C$_2$H$_5$O$_2$N) 1.36 mol.L^{-1} at room temperature. Through mass loss measurements the corrosion rate (CR), expressed in mm per year, was calculated using the following Equation 1[25]:

$$CR = \frac{K \cdot W}{A \cdot T \cdot D}$$ (1)

where K = constant (for CR mm/year, K=8.76 x 104); W = mass loss (g); A = exposed area (cm^2); T = duration of exposure (h); D = Ni-Mo density (g.cm^{-3}).

Table 1. Reagent concentrations in the Ni-Mo electrodeposition bath[10].

Reagent	Concentration (g.L^{-1})	Function
Nickel (II) Sulfate (NiSO$_4$)	52.60	Nickel Source
Sodium Citrate (Na$_3$C$_6$H$_5$O$_7$.2H$_2$O)	88.23	Improve conductivity and deposition speed
Sodium Molybdate (Na$_2$MoO$_4$)	9.68	Molybdenum Source

Electrochemistry test system (AUTOLAB potentiostat/galvanostat model PGSTAT100, controlled by NOVA 1.11 software) containing a conventional three–electrode cell was applied to carry out potentiodynamic polarization tests and electrochemical impedance spectroscopy. Saturated Calomel - Hg$_2$ | Hg$_2$Cl$_2$ electrode as reference electrode and graphite as counter electrode were used. Samples were kept in the electrolyte for 180 s before doing electrochemical experiments. The potentiodynamic polarization curves were recorded at a scan rate of 10 mV.s^{-1} in the range of –0.57 to -0.27 V versus SCE. EIS measurements were performed with an amplitude of 10 mV vs. SCE in the frequency range of 100 kHz-10 mHz.

The galvanostatic deposition efficiency (%E)[27] was evaluated by the ratio between the Ni-Mo electroplated mass and the theoretical mass (Equation 2):

$$\%E = \left(\frac{m_r}{m_c}\right) x100$$ (2)

where: m_r is the measured Ni-Mo mass gain, and m_c is the theoretical mass gain, calculated by Equation 3:

$$mc = \frac{t_i.M_i.I}{n_i.C_i.F}$$ (3)

Where: t_i is the deposition time (second), I is the total current passed (amperes), n_i is the number of electrons transferred per atom of metal, C_i is the weight fraction, M_i is the atomic mass of that element (g.mol^{-1}), ad F is Faraday`s constant (96,485 C.mol^{-1}).

Using Faraday's law, the m$_c$ is related with the thickness of the coating by Equation 4:

$$t = \frac{m_c}{D.S}$$ (4)

where t is the film thickness, (5 µm); D is the Ni-Mo density (g.cm^{-3}); S is the electrodeposition surface, (2.01 cm^2).

The structure of Ni-Mo coatings was analyzed using X–ray diffraction (X-ray diffractometer brand SHIMADZU model XRD-6000, with CuKα radiation (40 kV and 40 mA). The dimension of the crystallites of the Ni-Mo coating were obtained by the Scherrer Equation 5[27].

$$d = \lambda /\left(\beta_t \cos\theta\right)$$ (5)

where d is the crystallite size; λ is the wavelength of the element used for the diffraction, β_t is a full width at half maximum (FWHM); and θ is the corresponding angle.

Morphology and chemical composition of Ni–Mo coatings were studied using a Scanning Electron Microscope (JSM - 6610LV, brand JEOL) equipped with energy dispersive X–ray spectrometer (EDS). Roughness of the coatings was analyzed by Olympus laser confocal microscope, model LEXT OLS 4100, with 200X objective lenses. Measurements

are made in each sample along its width, in total three measurements, and in tribology by definition, the surface presents peaks (highest region) and valleys (deepest region). Therefore, the total roughness is the largest measured that comprises from the highest peak to deepest valley of the surface and the average roughness is the value calculated between the measures of the peaks and valleys.

The microhardness tests were performed using the Model Shimazdu microdurometer - HMV series, with a displacement ± 12.5 mm (0 to 25 mm) for both axes (X and Y), movement speed of up to 2 mm / s and positioning accuracy between 0.02 - 10 mm. The tests were carried out using Vickers indenter at 50 g load (15 second duration).

3. Results and Discussion

3.1. Effect of the addition of glycerol on the morphology and roughness of the Ni-Mo coating

Figure 1 shows the morphological characterization by SEM of Ni-Mo coating obtained in the absence (Figure 1a) and the presence (Figure 1b, 1c, 1d) of different amounts of glycerol. These micrographs revealed that the coating exhibits a nodular morphology, which is expected for the coatings with Mo contents analyzed in the present work[4].

The micrographs in Figure 1 indicate that glycerol influences the morphology of Ni-Mo coating. It is observed that in the absence of glycerol, there is a significant number of pores which decrease significantly with the addition of glycerol. It is also observed that in the coatings obtained in the presence of glycerol, the region of the coating surface formed by more uniform grains becomes broader with the increase in the amount of glycerol.

The SEM micrographs do not clearly show the effect of the glycerol on the coating compactness. To verify this effect, measurements of roughness were made in Ni-Mo coatings obtained in the absence and presence of glycerol. The roughness values of Ni-Mo coatings in the absence and presence of various glycerol contents are listed in Table 2. These show that the addition of glycerol decreases the roughness of the Ni-Mo coating, and this effect is more significant with increasing glycerol content. These results indicate that the presence of this additive results in a more compact deposit[28,29].

The EDS spectra of Ni-Mo coatings obtained in the presence and absence of different concentrations of glycerol are shown in Figure 2. These spectra include the presence of Fe from the substrate. To obtain a better reliability of analysis, Ni and Mo concentrations were calculated in the absence of Fe, and these results are shown in Table 3. These results show that in the absence and presence of glycerol up to a content of 0.27 mol.L⁻¹, the Mo concentration in the coating varies between 18.2 wt.% to 19.1 wt.%, and it is not clear how the addition of glycerol affects the Mo concentration in the coating. However, with the increased

Table 2. Roughness values of Ni-Mo coatings obtained in the absence and presence of various glycerol contents.

Glycerol concentration (mol.L⁻¹)	Average roughness (µm)	Total roughness (µm)
0.0	0.07	0.97
0.07	0.04	0.41
0.27	0.04	0.38
0.82	0.03	0.23
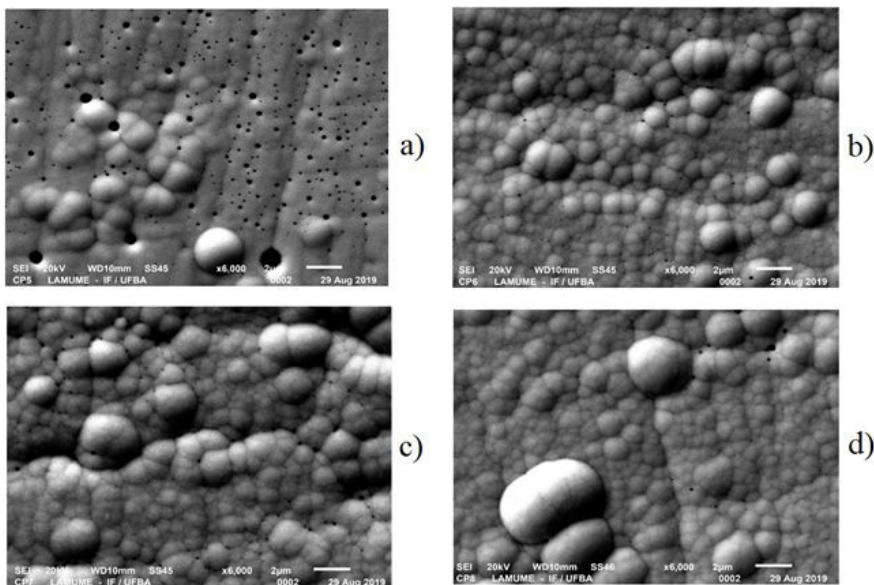
Figure 1. SEM micrographs of Ni-Mo coating obtained in the presence (b, c, d) and absence (a) of different glycerol contents. (b) 0.07 mol.L⁻¹, (c) 0.27 mol.L⁻¹, (d) 0.82 mol.L⁻¹.
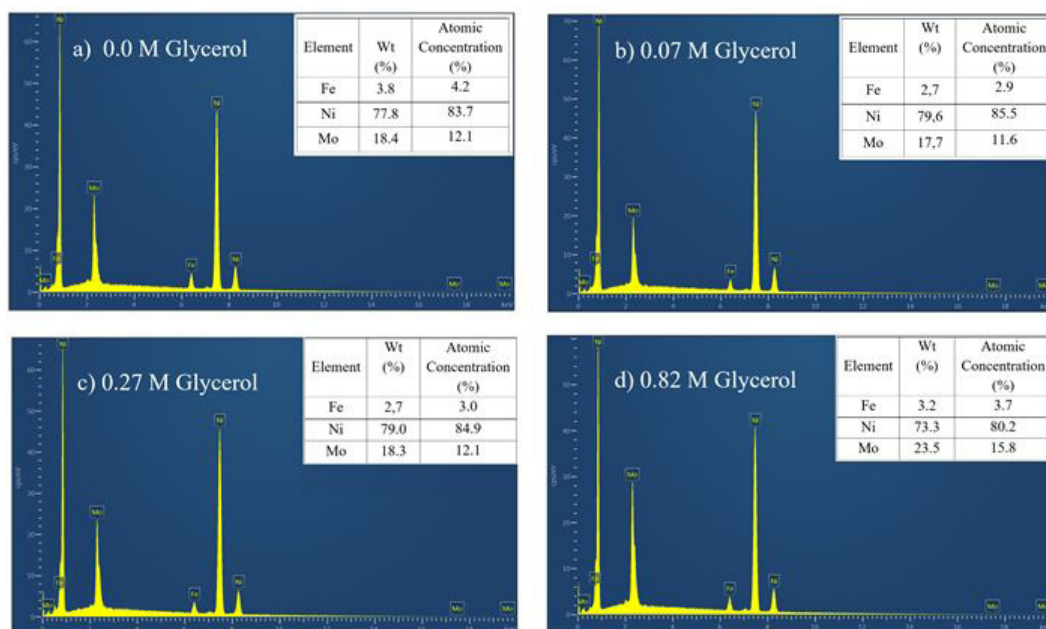
Figure 2. EDS spectrum of Ni-Mo coatings obtained in the absence and presence of different glycerol concentrations.

Table 3. Concentration of Ni and Mo in the layer volume of Ni-Mo coating obtained in the absence and presence of various glycerol contents.

Glycerol concentration (mol.L^{-1})	Ni concentration (wt%)	Mo concentration (wt%)
0.0	80.9	19.1
0.07	81.8	18.2
0.27	81.1	18.9
0.82	75.7	24.3

glycerol content to 0.82 mol.L^{-1} the Mo content in the coating increases to 24.3 wt.%.

The effect of glycerol on the morphology and roughness of Ni-Mo coating indicates that the glycerol is potentially adsorbed on the surface of the cathode during the electrodeposition process. Organic compounds are adsorbed onto the coating obtained by electrodeposition through free electrons. These electrons interact with the metallic substrate and with the coating being formed, thus allowing the adsorption of glycerol[30]. In Figure 3, the molecular structure of glycerol is shown and carbon atoms form bonds with hydroxyl groups. It is possible that the presence of free electrons in the hydroxyl allows the adsorption of glycerol in the Ni-Mo coating.

3.2. Evaluation of the addition of glycerol on the physical structure of the Ni-Mo coating

Figure 4 shows the diffractograms obtained for Mo-Ni coatings obtained in the absence and presence of varying concentrations of glycerol.

The XRD pattern of Ni-Mo coatings in Figure 4 exhibits the planes (111), (200), and (220), which correspond to the face-centered-cubic Ni-Mo solid solution phase[4,22].
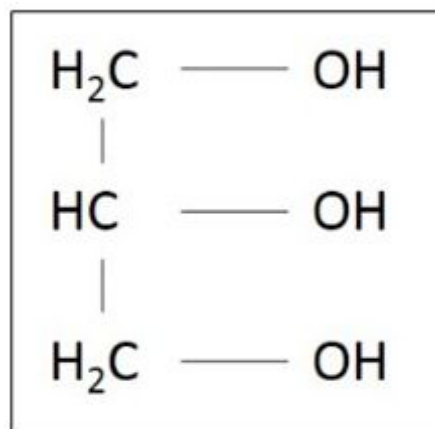
Figure 3. Molecular structure of glycerol.

The absence of peaks corresponding to Mo indicates the presence of a solid solution with Mo atoms dissolved in the lattice of Ni. The diffractograms in Figure 4 show that the peak corresponding to Ni (111) is the one that exhibits the highest intensity, which indicates that both in the absence and in the presence of glycerol the coatings present texture with the same preferred orientation.

Figure 4 also shows a peak that indicates the presence of carbon in the coating, introduced by the addition of glycerol. This presence can promote the formation of an amorphous structure. However, it has been observed[26] that the addition of glycerol in the Ni deposition bath in the same concentrations used in the present work does not change the width of the XRD pattern peaks, which is typical of a crystalline structure. Therefore, this behavior shows that

the presence of carbon, unlike Mo, does not promote the amorphization of Ni coating.

The results obtained from XRD pattern are consistent with SEM analysis. The presence of Ni and Fe detected from XRD pattern is confirmed by SEM analysis. The presence of Mo is detected through SEM analysis, and the absence of peaks corresponding to Mo in the XRD pattern is due to the presence of a solid solution with the atoms of that element dissolved in the lattice of Ni. Regarding the carbon detected in the XRD pattern the sensitivity of the equipment used in the SEM analysis was not sufficient to detect the presence of this element in the coating.

Table 4 shows the values of the size of crystallites in the absence and presence of different levels of glycerol. These values were determined from Equation 5, using the FWHM corresponding to peak Ni (111). With the addition of glycerol, these peaks widen and, consequently, the size of the crystallites decreases. This could be related to the decrease in grain size[31], indicating, therefore, that the addition and increase in glycerol content causes grain refining. Grain refining caused by the addition of glycerol has also been reported in Zn[23] and Zn-Ni[24] coatings.

According to Figure 4, the diffraction peak angle (2θ) of peak Ni (111) of Ni-Mo coatings obtained in the absence and presence of 0.07, 0.27 and 0.87 M of glycerol were found to be

43.73, 43.82, 43.93 and 44.04 degree, respectively. This increase in diffraction peak angle indicates an increase in tensile stress in Ni-Mo coatings with the addition of glycerol[10]. However, this increase in tensile stress is not enough to lead to the appearance of microcracks, as can be seen in SEM images (Figure 2).

3.3. Effect of glycerol addition on corrosion resistance of Ni-Mo coating

3.3.1. Mass loss measurements

Tables 5 and 6 show the values of the corrosion rate obtained from the mass loss tests of the Ni-Mo coatings obtained in the absence and presence of different concentrations of glycerol. The results corresponding to different immersion times in 0.5 mol.L^{-1} NaCl and 0.5 mol.L^{-1} NaOH solutions are shown in Tables 5 and 6 respectively. According to these results, the

Table 4. Effect of glycerol addition on Ni-Mo coating mean crystallites size in the absence and presence of different glycerol concentrations

Glycerol Content (mol.L^{-1})	Average crystallites size Ni-Mo (nm)
0	6.72
0.07	6.50
0.27	6.19
0.82	6.13
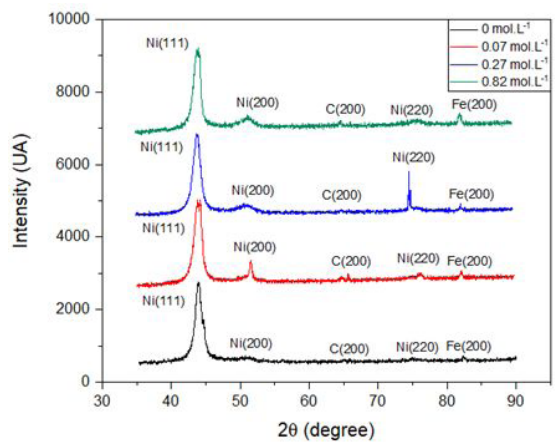
Figure 4. XRD pattern for Ni-Mo coatings obtained in the absence and presence of different glycerol concentrations.

Table 5. Corrosion rate of Ni-Mo coatings as a function of time for 0.5 mol.L^{-1}NaCl corrosive medium in the absence and presence of various glycerol concentrations.

Glycerol Content (mol.L^{-1})	Corrosion rate (mm/year)								
	24 h			48 h			72 h		
	Average	Highest value	Lower value	Average	Highest value	Lower value	Average	Highest value	Lower value
0	0.12555	0.13264	0.11594	0.09473	0.09727	0.09044	0.09062	0.10101	0.0804
0.07	0.12111	0.12983	0.10918	0.08938	0.09477	0.08378	0.08508	0.09325	0.07798
0.27	0.11792	0.12547	0.10699	0.08764	0.09164	0.08289	0.08273	0.08979	0.07541
0.82	0.11155	0.11548	0.10566	0.07599	0.0821	0.06896	0.07674	0.08395	0.06784

Table 6. Corrosion rate of Ni-Mo coatings as a function of time for 0.5 mol.L^{-1} NaOH corrosive medium in the absence and presence of various glycerol concentrations.

Glycerol Content (mol.L^{-1})	Δm /A (g/cm^2)								
	24 h			48 h			72 h		
	Average	Highest value	Lower value	Average	Highest value	Lower value	Average	Highest value	Lower value
0	0.02454	0.0279	0.0215	0.01906	0.02156	0.01856	0.01562	0.01753	0.01424
0.07	0.01973	0.02185	0.01766	0.0165	0.01871	0.01404	0.0138	0.01589	0.01169
0.27	0.01864	0.02057	0.01528	0.01632	0.01753	0.01253	0.01284	0.01513	0.01153
0.82	0.01538	0.01656	0.01419	0.01103	0.01419	0.00828	0.00965	0.01165	0.00915

addition of 0.82 mol.L^{-1} glycerol decreases the corrosion rate in both the acidic (pH 6) solution of 0.5 mol.L^{-1} NaCl and the alkaline solution (pH 13) NaOH 0.5 mol.L^{-1}, indicating increased corrosion resistance. However, the effect of the addition of 0.07 and 0.27 mol.L^{-1} of glycerol on the corrosion rate is unclear as the results are within the margin of error. Despite this, the results indicate a decrease in corrosion resistance in the alkaline solution with the addition of glycerol concentrations.

3.3.2. Potentiodynamic polarization measurement

In order to investigate the effect of glycerol addition on the corrosion resistance of the Ni - Mo coating potentiodynamic polarization curves were obtained. Through these curves the polarization resistance, corrosion current density (Icor), and corrosion potential (Ecor) were determined.

Figures 5 and 6 show the potentiodynamic polarization curves of Ni-Mo coatings obtained in the absence and presence of glycerol. Figures 5 and 6 correspond respectively to the curves obtained in 0.5 mol.L^{-1} NaCl and 0.5 mol.L^{-1} NaOH solutions. These figures show that in the anodic region of the curves obtained in both NaCl solution and NaOH solution, the current density decreases with the addition of glycerol and this decrease is more pronounced with the increase in the concentration of glycerol. This indicates the inhibition of Ni-Mo coating dissolution with the addition of glycerol.

The values of Rp, Icor and Ecor of Ni-Mo coatings obtained in the absence and presence of different glycerol concentrations are shown in Tables 7 and 8. Results corresponding to 0.5 mol.L^{-1} NaCl and 0.5 mol.L^{-1} NaOH solutions are shown in Tables 7 and 8, respectively. They show that both NaCl and NaOH solution Rp and Ecor values increase while Icor decreases with the addition of glycerol. This behavior indicates the increase in corrosion resistance with the addition of glycerol, which is more significant with increasing additive concentration.

3.3.3. Electrochemical Impedance Spectroscopy (EIS)

Figures 7 and 8 show the diagrams obtained by EIS in solution of 0.5 mol.L^{-1} NaCl and 0.5 mol.L^{-1} NaOH, respectively, for Ni-Mo coatings obtained in the absence and presence of glycerol. The experimental data were analyzed
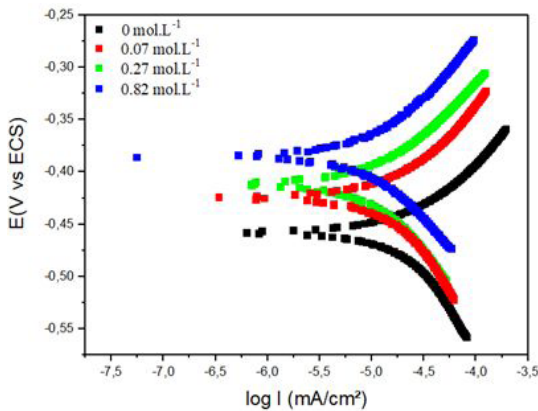
Figure 5. Potentiodynamic polarization curves in NaCl 0.5 mol.L^{-1} solution in the absence and presence of different glycerol concentrations.
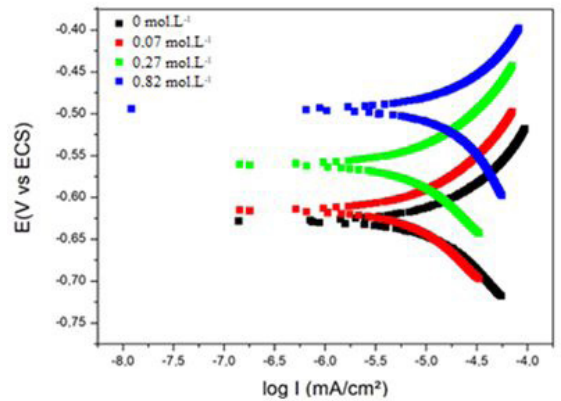
Figure 6. Potentiodynamic polarization curves in NaOH 0.5 mol.L^{-1} solution in the absence and presence of different glycerol concentrations.

Table 7. Ni-Mo coatings Rp, icor, and Ecor values in NaCl 0.5 mol.L^{-1} solution of Ni-Mo coatings obtained in the absence and presence of different glycerol content.

Glycerol Content (mol.L^{-1})	E(V vs ECS)	Rp (kΩ)	i_{cor} (μA.cm^{-2})
0	-0.458	1.072	10.532
0.07	-0.424	1.131	8.675
0.27	-0.412	1.965	4.954
0.82	-0.386	2.151	3.557

Table 8. Ni-Mo coatings Rp, icor, and Ecor values in NaOH 0.5 mol.L^{-1} solution of Ni-Mo coatings obtained in the absence and presence of different glycerol content.

Glycerol Content (mol.L^{-1})	Ecor(V vs ECS)	Rp (kΩ)	i_{cor} (μA.cm^{-2})
0	-0.628	3.233	2.282
0.07	-0.615	2.829	2.325
0.27	-0.562	7.178	0.628
0.82	-0.494	15.017	0.226
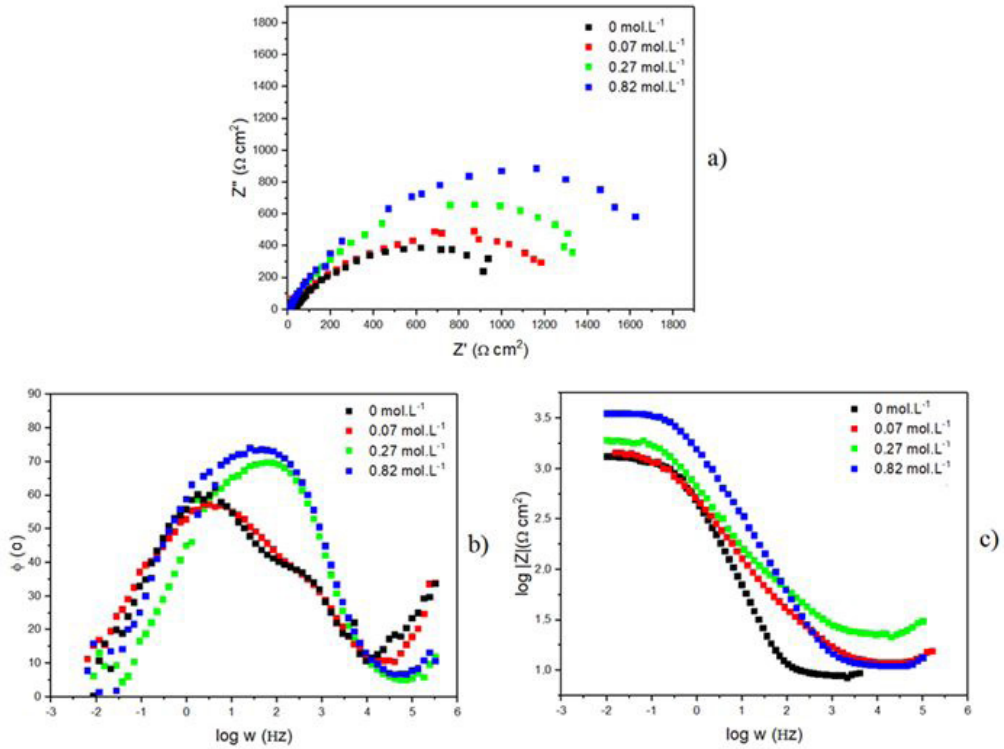
Figure 7. EIS diagrams in NaCl 0.5 mol.L⁻¹solution of Ni-Mo coating obtained in the absence and presence of different glycerol concentrations. a) Nyquist plot; b) Bode plot phase angle; c) Bode plot impedance module.
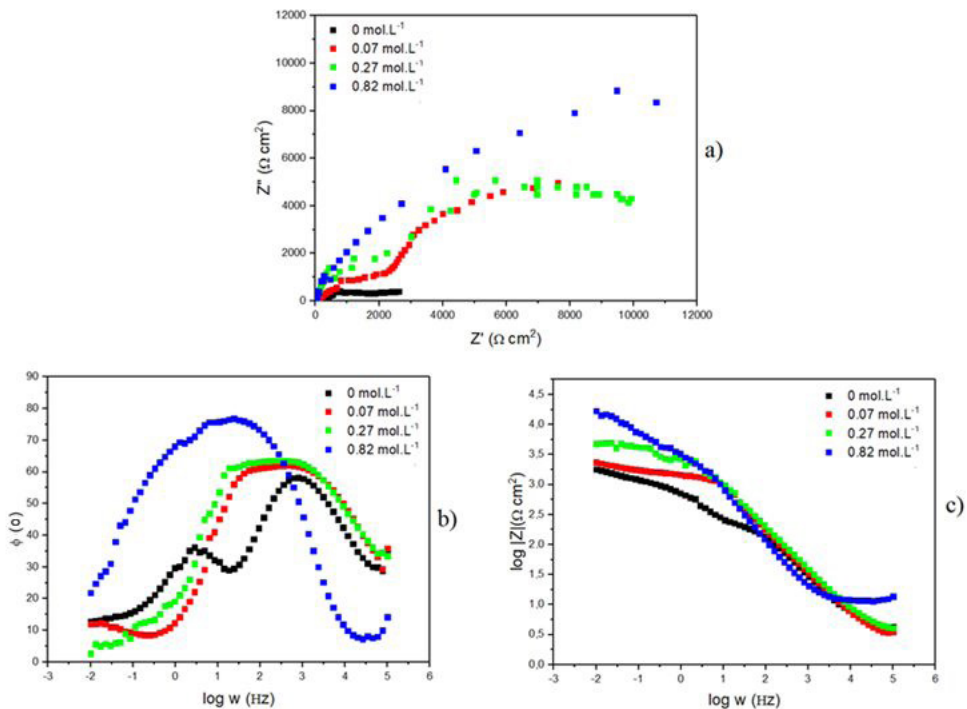
Figure 8. EIS diagrams in NaOH 0.5 mol.L⁻¹ solution of Ni-Mo coating obtained in the absence and presence of different glycerol concentrations. a) Nyquist plot; b) Bode plot phase angle; c) Bode plot impedance module.

according to the equivalent circuit model shown in Figure 9. In this equivalent circuit the constant phase element (CPE) was used instead of the capacitor (C) which allows obtaining a more accurate fitting[32]. The results obtained indicate that the equivalent circuit used allowed to clearly analyze the effect of the addition of glycerol on the corrosion resistance of Ni-Mo coating in both acidic and alkaline solutions.

Nyquist diagrams in Figures 7a and 8a are semicircle shaped indicating that corrosion in both the acidic NaCl solution and the alkaline NaOH solution is controlled by activation[18]. The control of the corrosive process by activation (load transfer), indicates that a necessary condition for the use of Icor to evaluate the corrosion resistance of the coating is met, since this parameter is determined from the Buttler-Volmer equation, which is only valid when the corrosive process is controlled by activation[33]. Figures 7a and 8a also show that the semicircle diameter increases with the addition of glycerol and this increase is greater with increasing additive concentration. A larger diameter of this semicircle indicates a higher polarization resistance, and consequently lower corrosion rate[34]. Therefore, Nyquist diagrams indicate improved corrosion resistance of Ni-Mo coating with the addition of glycerol and increasing the concentration of this additive in both acid and alkaline solutions.

Figures 7b, 7c, 8b, 8c, shows the Bode ($\log |Z|=f(\log \omega)$) and $\phi=f(\log \omega)$ impedance diagrams in 0.5 mol.L^{-1} NaCl (Figures 7b and 7c) and 0.5 mol.L^{-1} NaOH (Figures 8b and 8c). Figures 7c and 8c exhibit two maximum phase lags, which indicates the presence of two time constants, which are related to the occurrence of corrosion /passivation on the Ni-Mo coating surface. These figures show that the maximum value of phase, $\log \omega$ range between -3 and 0, increases with the addition of glycerol, which indicates that the presence of this additive improves the stability of the passive film formed in the Ni-Mo coating, both in the acidic and alkaline solution[32].

It has been found[35] that in Ni-Mo coating in NaCl solution there is the presence of a passive film consisting of Mo oxide located at the film / metal interface, and by Ni oxide / hydroxide located in the outer layer of the passive film. To analyze the effect of glycerol on the passive film of Ni-Mo coating, it is necessary to evaluate the behavior of the passive film after different immersion times in the corrosive solution. However, the Bode diagrams in Figures 7c and 8c indicate that the addition of glycerol tends to favor the protective capacity of the passive Ni-Mo coating film.

The maximum value of ϕ in Figures 7b and 8b shift increases with increasing glycerol content in the composite layer up to a maximum at coating obtained in the presence of 0.82 mol.L^{-1}, which indicates enhanced stability for the composite film[9]. Moreover, these figures show that for the coating obtained in the presence of 0.82 mol.L^{-1} there is a wider range of independence of the phase angle value from the logarithm of angular frequency compared to the other coatings. This wider range of independence of $\phi=f(\log \omega)$ implies that the coating obtained in the presence of 0.82 M is more corrosion resistant[36].

The results obtained through EIS are consistent with the results concerning the Rp, i_{cor}, and Ecor, and with the qualitative analysis of the potentiodynamic polarization curves of E vs. logI, which show that the addition of glycerol increases the corrosion resistance of Ni-Mo coating at both acidic and alkaline pH, and that this improvement is more significant with increasing glycerol content. These results are consistent with those obtained by mass loss measurements which show that the highest corrosion resistance of Ni-Mo coating is obtained with the addition of 0.82 mol.L^{-1} glycerol. Unlike the electrochemical tests, through the mass loss measurements it was not possible to clearly differentiate the effect of the 0.07 and 0.27 mol.L^{-1} contents due to the lower precision of these tests.

The improvement of corrosion resistance of the Ni-Mo coating with the addition of glycerol in the electrodeposition bath is related to the effect of this additive on the morphology and composition of the coating. The roughness measurements show that the addition of glycerol promotes the formation of a Ni-Mo coating with lower roughness, which implies a smaller contact area between the coating and the corrosive environment resulting in increased corrosion resistance. The increase in glycerol concentration tends to coat with less roughness, which favors the increase in corrosion resistance. Decreasing the porosity of Ni-Mo coatings with the addition of glycerol, as observed by SEM micrographs, also contributes to increased corrosion resistance.

By increasing the glycerol content from 0.27 to 0.82 mol.L^{-1} as can be seen from Figure 2, the Mo content in the coating increased from 18.6 wt% to 23 wt%. which probably contributed to the higher corrosion resistance of the coating obtained in the presence of 0.82 mol.L^{-1}. As mentioned in the introduction, the increased corrosion resistance of Ni-Mo coating with increasing Mo concentration is attributed to the increased protective capability of the passive film.
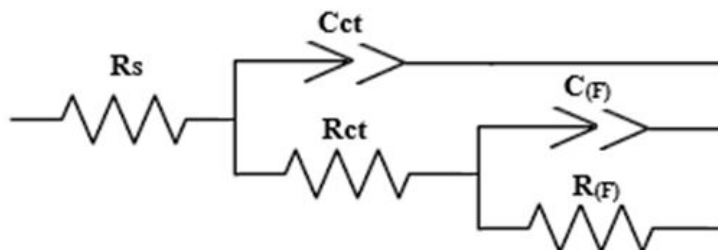
Figure 9. Equivalent circuit for impedance analysis where Rs: solution resistance, Cct: constant phase element, Rct: charge transfer resistance, C$_{(F)}$: capacitance of the coating, R$_{(F)}$: resistance of the coating.

There is also an optimum content of Mo from which the corrosion resistance of Mo-Ni coating starts to decrease with the increase in this additive. This is attributed to the effects of increased internal tension and grain refining caused by the addition of Mo, which becomes predominant from a certain critical Mo content. In the Ni-Mo coating analyzed in the present work, the greater the internal tension and the refining of the grains caused by the addition of glycerol were not sufficient to affect the corrosion resistance of the coating, which indicates that the Mo content in the analyzed coatings is below the critical content. Therefore, in this condition, the roughness effect caused by the addition of glycerol predominates.

The results obtained in the present work through electrochemical tests and loss mass measurements show that the addition of glycerol increases the corrosion resistance of Ni-Mo coating in both acid and alkaline environments. The corrosion resistance of Mo-Ni coatings is generally evaluated in acidic NaCl solution, however, it is also important to evaluate the corrosion resistance of this coating in alkaline solutions. Ni-Mo coatings are well known for their use as cathodes for hydrogen production from water by electrolysis in sodium hydroxide solutions[37]. Therefore, it is important that this coating is stable in an alkaline medium. Future work will investigate the effect of the addition of glycerol on the ability of an Ni-Mo coating to produce hydrogen in alkaline environments.

3.4. Effect of glycerol addition on deposition current efficiency of Ni-Mo coating

The effects of glycerol addition in the electrodeposition bath on the current efficiency (CE) and on the energy consumption of the Ni-Mo coating electroplating process are shown in Figure 10 and in Table 8, respectively. The current efficiency is less than 100%, which indicates that a hydrogen evolution reaction is occurring in parallel with Ni-Mo deposition.

Figure 10 shows that the addition of 0.82 mol.L^{-1} glycerol increases the CE of Ni-Mo coating in comparison with electrodeposition without glycerol. However, the effect of the addition of 0.03 and 0.07 mol.L^{-1} glycerol is unclear since the CE values are within the margin of error.
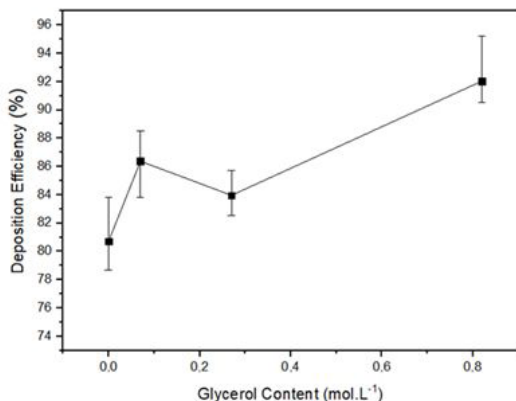
Figure 10. Effect of glycerol addition on current efficiency of Ni-Mo coating.

The results obtained in the present work and the previous study[23,24] indicate that the effect of the addition of glycerol on the CE of electroplated coatings depends on the coating composition. It was found[24] that the addition of 0.07 and 0.27 mol.L^{-1} glycerol increases the current efficiency (CE) of a Zn-Ni electrodeposit when compared with electrodeposition without glycerol, and the CE decreases the higher the glycerol content. However, in relation to Zn coating deposition, it was found[19] that the addition of glycerol decreases CE regardless of the amount of glycerol. Decreased CE due to the addition of glycerol is attributed to the formation of a strongly adsorbed layer that inhibits zinc electroreduction and consequently reduces the CE[24].

The CE elevation of the electrodeposition process caused by the presence of glycerol may be related to the increase of the bath deposition ionic conductivity and / or the inhibition of hydrogen evolution. This reaction is concurrent with the reduction reaction of metal cations and its inhibition thus favors the elevation of CE. In the present work the addition of glycerol did not cause a significant change in the deposition bath conductivity, therefore it is likely that the CE increase with the addition of 0.82 mol.L^{-1} glycerol is related to the inhibition of hydrogen evolution. As seen in item 3.1, the addition of glycerol decreases the presence of pores in the Ni-Mo coating. These pores act as atomic storage sites for H which act as active sites of the evolution of hydrogen. Therefore, it is possible that with the addition of 0.82 mol.L^{-1} glycerol, the decrease in the presence of pores was sufficient to inhibit hydrogen evolution to a level that enables higher CE . From the deposition efficiency results, the energy consumption values were obtained in the deposition process in the absence and presence of different glycerol concentrations. These values, shown in Table 9, show that the addition of 0.82 mol.L^{-1} glycerol results in a reduction in the energy consumption of at least 10.84% when compared to the absence of this additive.

3.5. Effect of glycerol addition on Ni-Mo coating hardness

Table 10 shows the Vickers microhardness measurement of Ni-Mo coatings obtained in the absence and the presence of different glycerol contents. The results in this table show that the hardness decreases with the presence of glycerol and this effect is more significant with the increase in the content of this additive.

As already mentioned, below a certain critical grain size with nanocrystalline dimension, the reverse Hall – Petch effect occurs, that is, the hardness starts to decrease with the grain refining. Considering that Liu et al.[10] found that this critical size corresponds to Ni-Mo coating crystallites with a dimension around 7.9 nm and the crystallites contained in the Ni-Mo coatings analyzed in the present work have a dimension less than 7 nm (Table 3), it is logical to assume that the investigated Ni-Mo coatings exhibit a grain size smaller than the critical size. Therefore, the decrease in hardness with the addition of glycerol can be attributed to the grain refining caused by the addition of this additive. The relationship between the size of the crystallites and the hardness of the coating obtained in the present work is consistent with the results obtained by Bigos et al.[38] who found

Table 9. Energy consumption values in the absence and presence of different glycerol co-concentrations.

Glicerol Content (mol.L^{-1})	Deposition efficiency (%)			Energy Consumption (kW.h/ton)		
	Average	Highest value	Lower value	Average	Highest value	Lower value
0	80.72	83.84	78.68	1090.17	1049.56	1118.51
0.07	88.54	92.38	83.81	993.85	952.60	1049.99
0.27	83.96	85.74	82.54	1048.06	1026.32	1066.12
0,82	90.54	95.21	87.04	971.90	924.25	1010.00

Table 10. Vickers microhardness of Ni-Mo coatings obtained in the absence and presence of different levels of glycerol and of Ni coating in the absence of glycerol.

Glycerol Content (mol.L^{-1})	Average (HV)	Highest value (HV)	Lower value (HV)
0.0 (Ni coating)[26]	749	770	706
0.0 (Ni-Mo coating)	1868	1958	1767
0.07	1718	1753	1684
0.27	1377	1456	1229
0.82	1377	1391	1352

that decreasing the size of the crystallites from 7nm to 5 nm results in a reduction in the hardness of the Ni-Mo coating.

The decrease in hardness with grain refining that occurs below a certain critical grain size is related to several mechanisms such as suppression of dislocation pile-ups[39], sliding in the grain boundaries (GB sliding)[40], and grain rotation[41]. The increase in the mechanical strength of a strengthening metal is based mainly on the dislocation pile-ups at grain boundary. Thus, the higher grain contour area with the grain refining favors the increase in hardness. However, below the critical grain size a suppression of dislocation pile-ups occurs because each individual grain will no longer be able to support more than one dislocation[39]. In crystalline materials, plastic deformation is based on nucleation and movement of dislocations. However, when the average grain size decreases below some critical value, the plastic deformation is controlled by GB-related deformation[40,41].

According to GB sliding the plastic deformation of the material with grains with a dimension smaller than the critical size occurs mainly in the form of a large number of small independent slip events in the grain boundaries. These slip events involve the movement of atoms with respect to each other. Below the critical size of the grain a significant fraction of the atoms is present in the grain boundary, and with the grain refining this presence increases, which favors the grain boundary sliding. Therefore, in this condition the grain refining favors the deformation of the material[42,43]. Through TEM, grain rotation during straining has been observed below the critical grain size. The grain rotation rate has been found to increase with decreasing grain size, thus favoring material deformation[44]. The decrease in hardness with grain refining is also attributed to the high volume fraction of the grain boundary triple junction below the critical grain size, which increases with decreasing grain size[45]. This behavior is related to the high disordered structure in the triple junction, however it is not clear how this characteristic affects the hardness of the material.

The decrease in the hardness of the Ni-Mo coating with the addition of glycerol tends to reduce its resistance to wear. This property is important in many applications,

however, the decrease in hardness caused by the addition of glycerol does not nullify the effect of the presence of Mo on the hardness of Ni-Mo coating. For comparison purposes, the Vickers microhardness of Ni coating was obtained and these values are shown in Table 10. These results show that even with the addition of glycerol, the hardness of Ni-Mo coating is significantly higher than Ni coating obtained in the absence of this additive. Therefore, it is possible that even with the decrease in hardness caused by the addition of glycerol, the Ni-Mo coating obtained in the presence of this additive can be used in several applications.

4. Conclusions

The corrosion resistance of the Ni-Mo coating in the 0.5 mol.L^{-1} NaCl acid solution and in the 0.5 mol.L^{-1} NaOH alkaline solution was found to increase with the addition of glycerol in bath electrodeposition, and this effect was found to be more intense with increasing glycerol concentration (0.07, 0.27 and 0.82 mol.L^{-1}).

The SEM observation and roughness measurements indicate that the addition of glycerol in the electrodeposition bath results in the presence of fewer pores and a more compact coating, which promotes corrosion resistance of the coating. The addition of 0.82 mol.L^{-1} in the bath deposition increases the Mo concentration in the Ni-Mo coating by 18 to 23% wt., which may have favored the increased corrosion resistance of the coating.

The hardness of the Ni-Mo coating decreases with the addition of glycerol, which may be related to the decrease in grain size, below a certain critical grain size. The addition of 0.82 mol.L^{-1} glycerol in the electrodeposition bath increases current efficiency and consequently reduces the amount of energy consumed during the Ni-Mo coating electrodeposition process.

5. Acknowledgment

Chemical Engineering, University Federal Bahia, Physical Metallurgy Laboratory – UFRGS, and the Coordenação de Aperfeiçoamento de Pessoal de Nível Superior – CAPES.

6. References

1. Prioteasa P, Anicai L, Visan T. Synthesis and corrosion characterization of electrodeposited Ni-Mo alloys obtained from aqueous solutions. UPB Sci Bull B Chem Mater Sci. 2010;72:11-24.

2. Bełtowska-Lehman E, Bigos A, Indyka P, Kot M. Electrodeposition and characterization of nanocrystalline Ni-Mo coatings. Surf Coat Tech. 2012;211:67-71.

3. Chassaing E, Portail N, Levy A-F, Wang G. Characterization of electrodeposited nanocrystalline Ni-Mo alloys. J Appl Electrochem. 2004;34(11):1085-91.

4. Laszczyńska A, Tylus W, Winiarski J, Szczygieł I. Evolution of corrosion resistance and passive film properties of Ni-Mo alloy coatings during exposure to 0.5 M NaCl solution. Surf Coat Tech. 2017;317:26-37.

5. Sanches LS, Domingues SH, Carubelli A, Mascaro LH. Electrodeposition of Ni-Mo and Fe-Mo alloys from sulfate-citrate acid solutions. J Braz Chem Soc. 2003;14(4):556-63.

6. Hu CC, Weng CY. Hydrogen evolving activity on nickel-molybdenum deposits using experimental strategies. J Appl Electrochem. 2000;30(4):499-506.

7. Hu W, Cao X, Wang F, Zhang Y. A novel cathode for alkaline water electrolysis. Int J Hydrogen Energy. 1997;22(6):621-3.

8. Arul Raj I, Venkatesan VK. Characterization of nickel molybdenum and nickel-molybdenum-iron alloy coatings as cathodes for alkaline water electrolysers. Int J Hydrogen Energy. 1988;13(4):215-23.

9. Ahmad YH, Tientong J, Nar M, D'Souza N, Mohamed AMA, Golden TD. Characterization and corrosion resistance of electrodeposited Ni-Mo-silicate platelet nanocomposite coatings. Surf Coat Tech. 2014;259:517-25.

10. Liu JH, Li WH, Pei ZL, Gong J, Sun C. Investigations on the structure and properties of nanocrystalline Ni-Mo alloy coatings. Mater Charact. 2020;167:110532.

11. Detor AJ, Miller MK, Schuh CA. Measuring grain-boundary segregation in nanocrystalline alloys: direct validation of statistical techniques using atom probe tomography. Philos Mag Lett. 2007;87(8):581-7.

12. Mosayebi S, Rezaei M, Mahidashti Z. Comparing corrosion behavior of Ni and Ni-Mo electroplated coatings in chloride mediums. Colloids Surf A Physicochem Eng Asp. 2020;594:124654.

13. Lima-Neto P, Correia AN, Vaz GL, Casciano PNS. Morphological, structural, microhardness and corrosion characterisations of electrodeposited Ni-Mo and Cr coatings. J Braz Chem Soc 2010;21(10):1968-76.

14. Mahidashti Z, Shahrabi T, Ramezanzadeh B. A new strategy for improvement of the corrosion resistance of a green cerium conversion coating through thermal treatment procedure before and after application of epoxy coating. Appl Surf Sci. 2016;390:623-32.

15. Halim J, Abdel-Karim R, El-Raghy S, Nabil M, Waheed A. Electrodeposition and characterization of nanocrystalline Ni-Mo catalysts for hydrogen production. J Nanomater. 2012;2012:1-9.

16. Bakhit B, Akbari A, Nasirpouri F, Hosseini MG. Corrosion resistance of Ni-Co alloy and Ni-Co/SiC nanocomposite coatings electrodeposited by sediment codeposition technique. Appl Surf Sci. 2014;307:351-9.

17. Bakhit B, Akbari A. Effect of particle size and co-deposition technique on hardness and corrosion properties of Ni-Co/SiC composite coatings. Surf Coat Tech. 2012;206(23):4964-75.

18. Huang P-C, Hou K-H, Wang G-L, Chen M-L, Wang J-R. Corrosion resistance of the Ni-Mo alloy coatings related to

19. coating's electroplating parameters. Int J Electrochem Sci. 2015;10:4972-84.

19. Niedbała J. Structure, morphology and corrosion resistance of Ni–Mo+PTh composite coatings. Bull Mater Sci. 2015;38(3):695-9.

20. Xu Y, Ma S, Fan M, Chen Y, Song X, Hao J. Design and properties investigation of NiMo composite coating reinforced with duplex nanoparticles. Surf Coat Tech. 2019;363:51-60.

21. Rezaeiolum A, Aliofkhazraei M, Karimzadeh A, Rouhaghdam AS, Miresmaeili R. Electrodeposition of Ni-Mo and Ni-Mo-(nano Al₂O₃) multilayer coatings. Surf Eng. 2018;34(6):423-32.

22. Jiang J, Feng C, Qian W, Zhu L, Han S, Lin H. Lin. Effect of graphene oxide nanosheets and ultrasonic electrodeposition technique on Ni–Mo/graphene oxide composite coatings. Mater Chem Phys. 2017;199:239-48.

23. Almeida MDJ, Rovere CAD, de Andrade Lima LRP, Ribeiro DV, Souza CAC. Glycerol effect on the corrosion resistance and electrodeposition conditions in a zinc electroplating process. Mater Res. 2019;22(4):1-13.

24. Gomes GA, Souza CAC, Carlos IA, de Andrade Lima LRP. Evaluation of the effect of deposition bath glycerol content on zinc nickel electrodeposits on carbon steel. Surf Coat Tech. 2019;206:2927-32.

25. Oliveira EM, Finazzi GA, Carlos IA. Influence of glycerol, mannitol and sorbitol on electrodeposition of nickel from a Watts bath and on the nickel film morphology. Surf Coat Tech. 2006;200(20-21):5978-85.

26. Costa JGR. Evaluation of glycerol as an additive in the electrodeposition of Ni and Ni-Mo [dissertation]. Salvador: Polytechnic School of the Federal University of Bahia; 2020.

27. Soares ME, Souza CAC, Kuri SE. Corrosion resistance of a Zn–Ni electrodeposited alloy obtained with a controlled electrolyte flow and gelatin additive. Surf Coat Tech. 2006;201(6):2953-9.

28. Holzwarth U, Gibson N. The Scherrer equation versus the 'Debye-Scherrer equation'. Nat Nanotechnol. 2011;6(9):534.

29. Park CJ, Lohrengel MM, Hamelmann T, Pilaski M, Kwon HS. Grain-dependent Passivation of Surfaces of Polycrystalline Zinc. Electrochim Acta. 2002;47(21):3395-9.

30. Mouanga M, Ricq L, Douglade G, Douglade J, Berçot P. Influence of coumarin on zinc electrodeposition. Surf Coat Tech. 2006;201(3-4):762-7.

31. Chassaing E, Portail N, Levy A, Wang G. Characterisation of electrodeposited nanocrystalline Ni–Mo alloys. J Appl Electrochem. 2004;34(11):1085-91.

32. Ahmad YH, Tientong J, Nar M, D'Souza N, Mohamed AMA, Golden TD. Characterization and corrosion resistance of electrodeposited Ni-Mo-silicate platelet nanocomposite coatings. Surf Coat Tech. 2014;259:517-25.

33. McCafferty E. Validation of corrosion rates measured by the Tafel extrapolation method. Corros Sci. 2005;47(12):3202-15.

34. Aguilar A, Sagüés A, Powers R. Powers, corrosion rates of steel in concrete. In: Berke NS, Chaker V, Whiting D, editors. ASTM-STP 1065. Philadelphia: American Society for Testing and Materials; 1990. p. 66-85.

35. Laszczyńska A, Tylus W, Winiarski J, Szczygieł I. Evolution of corrosion resistance and passive film properties of Ni-Mo alloy coatings during exposure to 0.5M NaCl solution. Surf Coat Tech. 2017;317:26-37..

36. Karolus M, Niedbała J, Rówi'nski EŁ, Agiewka E, Budniok A. Preparation of the electrodeposited Ni-Mo alloys with polymers. J Achiev Mater Manufact Eng. 2006;16(1-2):25-9.

37. Shetty S, Mohamed Jaffer Sadiq M, Bhat DK, Hegde AC. . Electrodeposition and characterization of Ni-Mo alloy as an electrocatalyst for alkaline water electrolysis. J Electroanal Chem. 2017;796:57-65.

38. Bigos A, Beltowska-Lehman E, Kot M. Studies on electrochemical deposition and physicochemical properties of nanocrystalline Ni-Mo alloys. Surf Coat Tech. 2017;317:103-9.

39. Hu J, Shi YN, Sauvage X, Sha G, Lu K. Grain boundary stability governs hardening and softening in extremely fine nanograined metals. Science. 2017;355(6331):1292-6.

40. Zhou X, Feng Z, Zhu L, Xu X, Miyagi L, Dong H, et al. High-pressure strengthening in ultrafine-grained metals. Nature. 2020;579(7797):67-72.

41. Zhou X, Tamura N, Mi Z, Lei J, Yan J, Zhang L, et al. Reversal in the size dependence of grain rotation. Phys Rev Lett. 2017;118(9):096101.

42. Schiøtz J, Di Tolla FD, Jacobsen KW. Softening of nanocrystalline metals at very small grain sizes. Nature. 1998;391(6667):561-3.

43. Yip S. The strongest size. Nature. 1998;391(6667):532-3.

44. Shan Z, Stach EA, Wiezorek JMK, Knapp JA, Follstaedt DM, Ma SX. Grain boundary-mediated plasticity in nanocrystalline nickel. Science. 2004;305(5684):654-7.

45. Yamasaki T, Schloβmacher P, Ehrlich K, Ogino Y. Formation of amorphous electrodeposited Ni-W alloys and their nanocrystallization. Nanostruct Mater. 1998;10(3):375-88.